Published in final edited form as:
Cell Metab. 2009 December ; 10(6): 491–498. doi:10.1016/j.cmet.2009.09.007.

Prevention of Steatosis by Hepatic JNK1

Guadalupe Sabio[1,2], **Julie Cavanagh-Kyros**[2], **Hwi Jin Ko**[2,4], **Dae Young Jung**[2,4], **Susan Gray**[2], **John Y. Jun**[4], **Tamera Barrett**[2], **Alfonso Mora**[2], **Jason K. Kim**[2,3,4], and **Roger J. Davis**[1,2,*]

[1] Howard Hughes Medical Institute, University of Massachusetts Medical School, Worcester, Massachusetts 01605, USA

[2] Program in Molecular Medicine, University of Massachusetts Medical School, Worcester, Massachusetts 01605, USA

[3] Department of Medicine, Division of Endocrinology, Metabolism and Diabetes, University of Massachusetts Medical School, Worcester, Massachusetts 01605, USA

[4] Department of Cellular and Molecular Physiology, Pennsylvania State University College of Medicine, Hershey, Pennsylvania 17033, USA

Abstract

Non-alcoholic steatosis (fatty liver) is a major cause of liver dysfunction that is associated with insulin resistance and metabolic syndrome. The cJun NH_2-terminal kinase 1 (JNK1) signaling pathway is implicated in the pathogenesis of hepatic steatosis and drugs that target JNK1 may be useful for treatment of this disease. Indeed, mice with defects in JNK1 expression in adipose tissue are protected against hepatic steatosis. Here we report that mice with specific ablation of *Jnk1* in hepatocytes exhibit glucose intolerance, insulin resistance, and hepatic steatosis. JNK1 therefore serves opposing actions in liver and adipose tissue to both promote and prevent hepatic steatosis. This finding has profound implications for the design of JNK1-selective drugs for the treatment of metabolic syndrome.

Introduction

Non-alcoholic fatty liver disease is the leading cause of liver dysfunction in the non-alcoholic, viral hepatitis-negative, population in the USA and Europe (Angulo and Lindor, 2002; Cortez-Pinto et al., 2006; Skelly et al., 2001). The disease represents a spectrum of liver pathologies, including steatosis, non-alcoholic steatohepatitis, and non-alcoholic cirrhosis. The incidence of non-alcoholic fatty liver disease is associated with obesity, dyslipidemia, insulin resistance, and type 2 diabetes (Anstee and Goldin, 2006). It is likely that this disease represents one aspect of metabolic syndrome (Marchesini et al., 2003; Sanyal, 2002).

*To whom correspondence should be addressed: Roger J. Davis, Howard Hughes Medical Institute, Program in Molecular Medicine, University of Massachusetts Medical School, 373 Plantation Street, Worcester, MA 01605, Telephone: (508) 856-6054, FAX: (508) 856-3210, Roger.Davis@Umassmed.Edu.
Present address: Departamento de Inmunología y Oncología, Centro Nacional de Biotecnología, CSIC. Campus de Cantoblanco-UAM, 28049-Madrid, Spain.

Supplemental Data: The Supplemental Data include Supplemental Experimental Procedures, Supplemental References, and thirteen Supplemental Figures and can be found online at http://

The cJun NH_2-terminal kinase 1 (JNK1) signaling pathway is implicated in the pathogenesis of metabolic syndrome (Weston and Davis, 2007). Thus, inhibitory phosphorylation of the adapter protein IRS1 by JNK1 can cause insulin resistance (Aguirre et al., 2000). Indeed, *Jnk1*$^{-/-}$ mice are protected against insulin resistance caused by feeding a high fat diet (HFD) (Hirosumi et al., 2002). This observation implicates JNK1 in the regulation of insulin resistance *in vivo*. However, *Jnk1*$^{-/-}$ mice exhibit resistance to HFD-induced obesity (Hirosumi et al., 2002). It is therefore possible that the effects of JNK1-deficiency on insulin resistance *in vivo* are a consequence of the failure of HFD-fed *Jnk1*$^{-/-}$ mice to develop obesity. Nevertheless, direct evidence demonstrating a role for JNK1 in the regulation of insulin resistance has been obtained from studies of mice with adipose-specific JNK1-deficiency that exhibit protection against HFD-induced insulin resistance and hepatic steatosis despite normal development of HFD-induced obesity (Sabio et al., 2008).

The liver represents a site of metabolic regulation by JNK1. Indeed, studies using adenoviral delivery of dominant-negative JNK (Nakatani et al., 2004) or *Jnk* shRNA (Yang et al., 2007) to the liver indicate that JNK1 plays an important role in negative regulation of hepatic insulin signaling. Furthermore, *Jnk1*$^{-/-}$ mice fed a methione and choline-deficient diet are less susceptible to hepatic steatosis (Schattenberg et al., 2006). Moreover, transgenic expression of the MAP kinase phosphatase DUSP-9 in the liver suppresses the activation of MAP kinases, including JNK, and increases insulin sensitivity (Emanuelli et al., 2008). Together, these data indicate that JNK1 plays a critical role in metabolic regulation of the liver. However, it is established that hepatic function, including steatosis and insulin resistance, can be regulated by JNK1 in adipose tissue (Sabio et al., 2008). The relative contribution of JNK1 in hepatocytes to the regulation of HFD-induced hepatic insulin resistance and steatosis is therefore unclear.

The purpose of this study was to test the role of hepatic JNK1. Our approach was to examine the effect of hepatocyte-specific ablation of the *Jnk1* gene in mice. Contrary to expectations, we found that these mice exhibit glucose intolerance, insulin resistance, and hepatic steatosis.

Results and Discussion

To test the role of JNK1 in the liver, we created mice without (L^{WT}) and with (L^{KO}) selective ablation of the *Jnk1* gene in hepatocytes (Figure 1A). Loss of hepatic JNK1 did not alter the expression of other JNK isoforms (Figure S1). Measurement of JNK activity demonstrated that a high fat diet (HFD) caused JNK activation in the liver and adipose tissue of control (L^{WT}) mice, but JNK activation was detected only in adipose tissue and not in liver of L^{KO} mice (Figure 1B). A JNK substrate site (Ser-307) that negatively regulates insulin receptor substrate (IRS)-1 (Aguirre et al., 2000) exhibited increased phosphorylation in the liver of HFD-fed L^{WT} mice, but not in L^{KO} mice (Figure 1C). Together, these data indicate that mice with hepatocyte-specific JNK1-deficiency represent a model for the analysis of the role of JNK1 in the liver.

Hepatocyte-specific JNK1-deficiency causes glucose intolerance

We anticipated that L^{KO} mice would exhibit protection against the deleterious effects of diet-induced obesity compared with L^{WT} mice. This expectation was based on previous studies that have established a role for JNK1 as an inhibitor of insulin signal transduction in multiple tissues (Aguirre et al., 2000; Hirosumi et al., 2002; Sabio et al., 2008). Moreover, studies using intravenous administration of adenovirus vectors to interfere with the JNK1 pathway in the liver suggest that hepatic JNK1 negatively regulates insulin signaling in the liver (Nakatani et al., 2004; Yang et al., 2007). In contrast, we found that HFD-fed L^{KO} and L^{WT} mice exhibited similar glucose intolerance (Figure S2A), insulin-induced decrease in blood glucose levels (Figure S2B), glucose-induced insulin release (Figure S2C), and serum glucose levels (Figure S3B,C). Furthermore, hyperinsulinemic-euglycemic clamp studies demonstrated a similar loss

of hepatic insulin action in HFD-fed L^{KO} and L^{WT} mice (Figure S3F). These data indicated that JNK1-deficiency in hepatocytes does not protect against diet-induced insulin resistance. Moreover, we found that chow-fed L^{KO} mice exhibited a profound defect in glucose-induced activation of hepatic AKT (Figure 1D), glucose intolerance (Figure 1E), and mild hyperglycemia (Figure 1F).

The observation that mice with hepatocyte-specific ablation of the *Jnk1* gene exhibit glucose intolerance (Figure 1E) contrasts with conclusions of previous studies of hepatic JNK1 that have employed intravenous delivery of adenoviruses that express dominant-negative JNK (Nakatani et al., 2004) or *Jnk* shRNA (Yang et al., 2007). The mechanism that accounts for the different phenotypes of these mouse models is unclear. One possibility is that these phenotypes reflect the effect of disruption of the JNK1 signaling pathway in different cell types. Thus, *Cre*-mediated ablation of *Jnk1* in hepatocytes may differ from the effect of adenovirus-mediated suppression of JNK1 signaling in multiple hepatic cell types, including hepatocytes, stellate cells, endothelial cells, and innate immune cells (e.g. Kupffer cells and NKT cells). Indeed, studies of murine hepatitis have established that the phenotype of mice with hepatocyte-specific ablation of *Jnk1* markedly differs from mice with ablation of *Jnk1* in multiple hepatic cell types (Das et al., 2009).

Hepatocyte-specific JNK1-deficiency increases insulin clearance

The major defect in glucose-induced hepatic insulin signaling observed in chow-fed L^{KO} mice (Figure 1D) may reflect a reduction in the blood concentration of insulin. No significant difference in the fasting blood insulin concentration between L^{KO} and L^{WT} mice was detected (Figure 2A). Morphological analysis demonstrated that the size of pancreatic islets was similar in L^{KO} and L^{WT} mice (Figure S4). Nevertheless, the amount of glucose-induced blood insulin was markedly decreased in L^{KO} mice compared with L^{WT} mice (Figure 2B). This loss of blood insulin could result from decreased insulin secretion or increased insulin clearance. To distinguish between these possible mechanisms, we examined the blood concentration of C-peptide (a proteolytic by-product of insulin processing) that is secreted together with insulin from pancreatic β-cells. We found that the fasting C-peptide concentration in the blood of L^{KO} mice was greatly increased compared with L^{WT} mice (Figure 2C). Nevertheless, a similar glucose-induced increase in blood C-peptide concentration was detected in L^{KO} and L^{WT} mice (Figure 2D), suggesting that insulin secretion was not altered in L^{KO} mice. Together, these observations suggest that insulin clearance was increased in L^{KO} mice compared with L^{WT} mice. To test this hypothesis, we injected mice with human insulin and measured the time course of changes in the concentration of human insulin in the blood. This analysis demonstrated that, compared with L^{WT} mice, the peak insulin concentration detected in L^{KO} mice was greatly reduced (Figure 2E). The clearance of blood insulin by L^{KO} mice was also markedly increased compared with L^{WT} mice (Figure 2E). Together, these data indicate that the normal levels of blood insulin detected in fasting L^{KO} mice are due to increased insulin clearance balanced by a compensatory increase in insulin secretion.

The liver is the major site of insulin clearance within the body. Indeed, it is estimated that 50% of insulin newly secreted by pancreatic β cells into the portal vein is internalized and degraded by the liver (Duckworth et al., 1998). Hepatic insulin clearance requires the insulin receptor (Michael et al., 2000) and is regulated by Ceacam1 (Poy et al., 2002). The increased amounts of insulin receptor and Ceacam1 in the liver (Figure 2F & S5) may contribute to the increased insulin clearance in L^{KO} mice (Figure 2E).

Hepatocyte-specific JNK1-deficiency causes insulin resistance

To further characterize the metabolic phenotype of chow-fed L^{KO} mice, we performed a hyperinsulinemic-euglycemic clamp study. This analysis demonstrated that L^{KO} mice

exhibited increased hepatic glucose production (HGP) during the clamp and therefore decreased hepatic insulin action compared with L^{WT} mice (Figure 3B,C). Indeed, the liver of L^{KO} mice expressed increased amounts of PGC-1α (Figure S6), a co-activator of the gluconeogenic gene transcription factors HNF4α and FOXO1 (Puigserver et al., 2003; Yoon et al., 2001). Basal HGP and insulin-stimulated whole body glucose turnover were not altered in L^{KO} mice (Figure 3A & 3D). The fat and lean mass of L^{WT} and L^{KO} mice were similar (Figure 3E,F). Insulin treatment caused similar JNK-independent (Rui et al., 2001) negative feed-back phosphorylation of IRS1 on Ser-307 in L^{KO} mice compared with L^{WT} mice (Figure 3I). However, decreased hepatic AKT activation was detected in L^{KO} mice compared with L^{WT} mice (Figure 3G,H). This reduction in AKT activation was associated with reduced insulin-stimulated tyrosine phosphorylation of the insulin receptor and IRS1 (Figure S7). Together, these data demonstrate that hepatic loss of JNK1 causes insulin resistance in liver.

Hepatocyte-specific JNK1-deficiency causes hepatic steatosis

The increased insulin clearance and hepatic insulin resistance phenotype of chow-fed L^{KO} mice compared with L^{WT} mice (Figures 2 & 3) is likely to cause profound metabolic consequences. Indeed, we found that chow-fed L^{KO} mice exhibited hepatic steatosis (Figure 4A) associated with increased accumulation of triglyceride (Figure 4B) and increased inflammation (Figure S8) compared with L^{WT} mice. Increased amounts of triglyceride were also detected in the blood of chow-fed L^{KO} mice (Figure S9). In contrast, HFD-fed L^{KO} and L^{WT} mice accumulated a similar amount of triglyceride in liver (Figure S10).

The increased triglyceride accumulation in chow-fed L^{KO} mice could be mediated by increased dietary lipid absorption, decreased fat oxidation, and/or increased lipogenesis. We found no differences between L^{KO} and L^{WT} mice in the respiratory exchange quotient $[V_{CO2}]/[V_{O2}]$ (Figure S11) or the intestinal absorption of dietary fat (Figure S12). The L^{KO} mice exhibited increased energy expenditure compared with L^{WT} mice, but no differences in food/water intake or physical activity in L^{KO} mice were detected (Figure S11). These observations do not support a role for increased dietary fat absorption or decreased fat oxidation as a cause of the hepatic steatosis in L^{KO} mice. *De novo* lipogenesis may therefore contribute to steatosis in L^{KO} mice. Indeed, increased lipogenesis was detected in the liver of chow-fed L^{KO} mice compared with L^{WT} mice (Figure 4C). Moreover, L^{KO} liver exhibited increased expression of genes that promote hepatic lipogenesis (*C/ebpα C/ebpβ Pgc-1β Pparγ*, and *Srebp1*) and also genes that encode enzymes that contribute to lipogenesis (*Acacα/β*, *Acot3*, *Acsl1/4*, *Dgat1*, *Fas*, and *Gyk*) and the export of triglyceride from the liver (*Mttp*) (Figure 4D). These changes in gene expression contribute to hepatic steatosis in chow-fed L^{KO} mice compared with L^{WT} mice. Furthermore, the increased expression of *C/ebpβ* in the liver of L^{KO} mice may contribute to enhanced insulin clearance by increasing insulin receptor expression (Foti et al., 2003) (Figure 2E,F).

Implications

Steatosis is a widespread human disease that can progress to steatohepatitis and liver failure (Angulo and Lindor, 2002; Cortez-Pinto et al., 2006; Skelly et al., 2001). The finding that the loss of JNK1 in hepatocytes causes steatosis identifies a possible complication of drug therapies involving JNK1 inhibition designed to treat insulin resistance. Indeed, the hepatic insulin resistance caused by hepatocyte-specific ablation of the *Jnk1* gene is associated with increased gluconeogenesis and also increased lipogenesis. This paradox (selective insulin resistance) represents a central characteristic of type 2 diabetes with suppression of the FOXO1 pathway and activation of the SREBP-1 pathway (Brown and Goldstein, 2008). These considerations indicate that hepatocyte-specific JNK1-deficient mice exhibit the typical features of insulin resistance that are associated with metabolic syndrome. The increased expression of the transcription factor FOXO1, the co-activator PGC-1α, and gluconeogenic target genes (e.g.

Pepck) may contribute to gluconeogenesis in L^{KO} mice (Figure S6). The mechanism that accounts for increased lipogenesis is unclear, but is most likely the result of increased expression of multiple lipogenic genes (Fig. 4E) and increased expression of lipogenic transcription factors (e.g. SREBP-1, C/EBPα/β, and PPARγ) and the co-activator PGC-1β (Fig. 4D).

Hepatic steatosis is prevented in *Jnk1*$^{-/-}$ mice (Schattenberg et al., 2006). This observation suggests that the metabolic milieu in response to JNK1-deficiency in different organs may compensate for the effects of JNK1-deficiency in hepatocytes. Indeed, JNK1 plays a major regulatory role in adipose tissue leading to protection against HFD-induced hepatic insulin resistance and steatosis (Sabio et al., 2008). This is consistent with the finding that systemic treatment of mice with a JNK inhibitor can protect against the effects of feeding a HFD (Kaneto et al., 2004). However, not all of the deleterious effects of hepatocyte-specific JNK1-deficiency are compensated in *Jnk1*$^{-/-}$ mice, including increased insulin clearance (Figure S13).

The observation that hepatic JNK1-deficiency increases insulin clearance has implications for the use of JNK1 as a drug target for the treatment of metabolic syndrome, including insulin resistance and steatosis. Disease progression from metabolic syndrome to type 2 diabetes is triggered by the failure of pancreatic β-cells due to exhaustion (Burks and White, 2001). In this regard, the compensatory increase in insulin secretion in response to enhanced insulin clearance caused by hepatic JNK1 inhibition may have adverse chronic effects on β-cell function. The cytoprotective effects of JNK inhibition on β cells (Bonny et al., 2001) may therefore be critical for the design of effective therapies that target JNK1 for the treatment of metabolic syndrome.

Experimental procedures

Mice

We have described *Jnk1*$^{-/-}$ mice (Dong et al., 1998), *Jnk1*$^{f/f}$ mice (Das et al., 2007), and *Jnk2*$^{-/-}$ mice (Yang et al., 1998). *Alb-Cre* mice (Postic et al., 1999) were obtained from the Jackson Labs. The mice were backcrossed to the C57BL/6J strain (Jackson Labs) and were housed in facilities accredited by the American Association for Laboratory Animal Care (AALAC). All studies were performed using male mice (8–24 wks old). The mice were genotyped by PCR analysis of genomic DNA (Das et al., 2007). The animal studies were approved by the Institutional Animal Care and Use Committees (IACUC) of the University of Massachusetts Medical School, University of Cincinnati, and Pennsylvania State University College of Medicine.

Immunoblot analysis

Tissue extracts were prepared using Triton lysis buffer [20 mM Tris (pH 7.4), 1% Triton X-100, 10% glycerol, 137 mM NaCl, 2 mM EDTA, 25 mM β-glycerophosphate, 1 mM sodium orthovanadate, 1 mM phenylmethylsulfonyl fluoride, and 10 μg/mL of aprotinin and leupeptin]. Extracts (20–50 μg of protein) and immunoprecipitates (prepared from 2–10 mg protein) were examined by protein immunoblot analysis. The antibodies employed were: AKT, phosphoSer-308 AKT, and phosphoSer-473 AKT (Cell Signaling); IRS1 (Sabio et al., 2008); IRS2, phosphotyrosine, and phospho-Ser^{307} IRS1 (Millipore); insulin receptor β sub-unit, JNK1 and GAPDH (Santa Cruz); and JNK1/2 (BD Pharmingen). Immunecomplexes were detected by enhanced chemiluminescence (NEN). Quantitation of immunoblots was performed using the Odyssey™ infrared imaging system (LI-COR Biosciences).

Measurement of blood glucose and insulin concentration

Blood glucose was measured with an Ascensia Breeze 2 glucose meter (Bayer). Insulin and insulin C-peptide in plasma were measured by ELISA using a Luminex 200 machine (Millipore).

Statistical analysis

Differences between groups were examined for statistical significance using the Student's test or analysis of variance (ANOVA) with the Fisher's test.

Supplementary Material

Refer to Web version on PubMed Central for supplementary material.

Acknowledgments

We thank D. Lee and P. Tso for the analysis dietary fat absorption (Mouse Metabolic Phenotyping Center, University of Cincinnati); M. Das for providing the floxed *Jnk1* mice, V. Benoit, J. Reilly, J-H. Liu, and R. Friedline for expert technical assistance; and K. Gemme for administrative assistance. These studies were supported by grants from the National Institutes of Health (CA65861 to R.J.D and DK80756 to J.K.K.) and the American Diabetes Association (7-07-RA-80 to J.K.K.). The UMass Mouse Phenotyping Center is supported by the NIDDK Diabetes and Endocrinology Research Center (DK52530). R.J.D. is an Investigator of the Howard Hughes Medical Institute.

References

Aguirre V, Uchida T, Yenush L, Davis RJ, White MF. The c-Jun NH(2)-terminal kinase promotes insulin resistance during association with insulin receptor substrate-1 and phosphorylation of Ser(307). J Biol Chem 2000;275:9047–9054. [PubMed: 10722755]

Angulo P, Lindor KD. Treatment of non-alcoholic steatohepatitis. Best Pract Res Clin Gastroenterol 2002;16:797–810. [PubMed: 12406446]

Anstee QM, Goldin RD. Mouse models in non-alcoholic fatty liver disease and steatohepatitis research. Int J Exp Pathol 2006;87:1–16. [PubMed: 16436109]

Bonny C, Oberson A, Negri S, Sauser C, Schorderet DF. Cell-permeable peptide inhibitors of JNK: novel blockers of beta-cell death. Diabetes 2001;50:77–82. [PubMed: 11147798]

Brown MS, Goldstein JL. Selective versus total insulin resistance: a pathogenic paradox. Cell Metab 2008;7:95–96. [PubMed: 18249166]

Burks DJ, White MF. IRS proteins and beta-cell function. Diabetes 2001;50(Suppl 1):S140–145. [PubMed: 11272176]

Cortez-Pinto H, de Moura MC, Day CP. Non-alcoholic steatohepatitis: from cell biology to clinical practice. J Hepatol 2006;44:197–208. [PubMed: 16274837]

Das M, Jiang F, Sluss HK, Zhang C, Shokat KM, Flavell RA, Davis RJ. Suppression of p53-dependent senescence by the JNK signal transduction pathway. Proc Natl Acad Sci U S A 2007;104:15759–15764. [PubMed: 17893331]

Das M, Sabio G, Jiang F, Rincon M, Flavell RA, Davis RJ. Induction of hepatitis by JNK-mediated expression of TNF-alpha. Cell 2009;136:249–260. [PubMed: 19167327]

Dong C, Yang DD, Wysk M, Whitmarsh AJ, Davis RJ, Flavell RA. Defective T cell differentiation in the absence of Jnk1. Science 1998;282:2092–2095. [PubMed: 9851932]

Duckworth WC, Bennett RG, Hamel FG. Insulin degradation: progress and potential. Endocr Rev 1998;19:608–624. [PubMed: 9793760]

Emanuelli B, Eberle D, Suzuki R, Kahn CR. Overexpression of the dual-specificity phosphatase MKP-4/DUSP-9 protects against stress-induced insulin resistance. Proc Natl Acad Sci U S A 2008;105:3545–3550. [PubMed: 18296638]

Foti D, Iuliano R, Chiefari E, Brunetti A. A nucleoprotein complex containing Sp1, C/EBP beta, and HMGI-Y controls human insulin receptor gene transcription. Mol Cell Biol 2003;23:2720–2732. [PubMed: 12665574]

Hirosumi J, Tuncman G, Chang L, Gorgun CZ, Uysal KT, Maeda K, Karin M, Hotamisligil GS. A central role for JNK in obesity and insulin resistance. Nature 2002;420:333–336. [PubMed: 12447443]

Kaneto H, Nakatani Y, Miyatsuka T, Kawamori D, Matsuoka TA, Matsuhisa M, Kajimoto Y, Ichijo H, Yamasaki Y, Hori M. Possible novel therapy for diabetes with cell-permeable JNK-inhibitory peptide. Nat Med 2004;10:1128–1132. [PubMed: 15448687]

Marchesini G, Bugianesi E, Forlani G, Cerrelli F, Lenzi M, Manini R, Natale S, Vanni E, Villanova N, Melchionda N, et al. Nonalcoholic fatty liver, steatohepatitis, and the metabolic syndrome. Hepatology 2003;37:917–923. [PubMed: 12668987]

Michael MD, Kulkarni RN, Postic C, Previs SF, Shulman GI, Magnuson MA, Kahn CR. Loss of insulin signaling in hepatocytes leads to severe insulin resistance and progressive hepatic dysfunction. Mol Cell 2000;6:87–97. [PubMed: 10949030]

Nakatani Y, Kaneto H, Kawamori D, Hatazaki M, Miyatsuka T, Matsuoka TA, Kajimoto Y, Matsuhisa M, Yamasaki Y, Hori M. Modulation of the JNK pathway in liver affects insulin resistance status. J Biol Chem 2004;279:45803–45809. [PubMed: 15331609]

Postic C, Shiota M, Niswender KD, Jetton TL, Chen Y, Moates JM, Shelton KD, Lindner J, Cherrington AD, Magnuson MA. Dual roles for glucokinase in glucose homeostasis as determined by liver and pancreatic beta cell-specific gene knock-outs using Cre recombinase. J Biol Chem 1999;274:305–315. [PubMed: 9867845]

Poy MN, Yang Y, Rezaei K, Fernstrom MA, Lee AD, Kido Y, Erickson SK, Najjar SM. CEACAM1 regulates insulin clearance in liver. Nat Genet 2002;30:270–276. [PubMed: 11850617]

Puigserver P, Rhee J, Donovan J, Walkey CJ, Yoon JC, Oriente F, Kitamura Y, Altomonte J, Dong H, Accili D, et al. Insulin-regulated hepatic gluconeogenesis through FOXO1-PGC-1alpha interaction. Nature 2003;423:550–555. [PubMed: 12754525]

Rui L, Aguirre V, Kim JK, Shulman GI, Lee A, Corbould A, Dunaif A, White MF. Insulin/IGF-1 and TNF-alpha stimulate phosphorylation of IRS-1 at inhibitory Ser307 via distinct pathways. J Clin Invest 2001;107:181–189. [PubMed: 11160134]

Sabio G, Das M, Mora A, Zhang Z, Jun JY, Ko HJ, Barrett T, Kim JK, Davis RJ. A stress signaling pathway in adipose tissue regulates hepatic insulin resistance. Science 2008;322:1539–1543. [PubMed: 19056984]

Sanyal AJ. AGA technical review on nonalcoholic fatty liver disease. Gastroenterology 2002;123:1705–1725. [PubMed: 12404245]

Schattenberg JM, Singh R, Wang Y, Lefkowitch JH, Rigoli RM, Scherer PE, Czaja MJ. JNK1 but not JNK2 promotes the development of steatohepatitis in mice. Hepatology 2006;43:163–172. [PubMed: 16374858]

Skelly MM, James PD, Ryder SD. Findings on liver biopsy to investigate abnormal liver function tests in the absence of diagnostic serology. J Hepatol 2001;35:195–199. [PubMed: 11580141]

Weston CR, Davis RJ. The JNK signal transduction pathway. Curr Opin Cell Biol 2007;19:142–149. [PubMed: 17303404]

Yang DD, Conze D, Whitmarsh AJ, Barrett T, Davis RJ, Rincon M, Flavell RA. Differentiation of CD4 + T cells to Th1 cells requires MAP kinase JNK2. Immunity 1998;9:575–585. [PubMed: 9806643]

Yang R, Wilcox DM, Haasch DL, Jung PM, Nguyen PT, Voorbach MJ, Doktor S, Brodjian S, Bush EN, Lin E, et al. Liver-specific knockdown of JNK1 up-regulates proliferator-activated receptor gamma coactivator 1 beta and increases plasma triglyceride despite reduced glucose and insulin levels in diet-induced obese mice. J Biol Chem 2007;282:22765–22774. [PubMed: 17550900]

Yoon JC, Puigserver P, Chen G, Donovan J, Wu Z, Rhee J, Adelmant G, Stafford J, Kahn CR, Granner DK, et al. Control of hepatic gluconeogenesis through the transcriptional coactivator PGC-1. Nature 2001;413:131–138. [PubMed: 11557972]

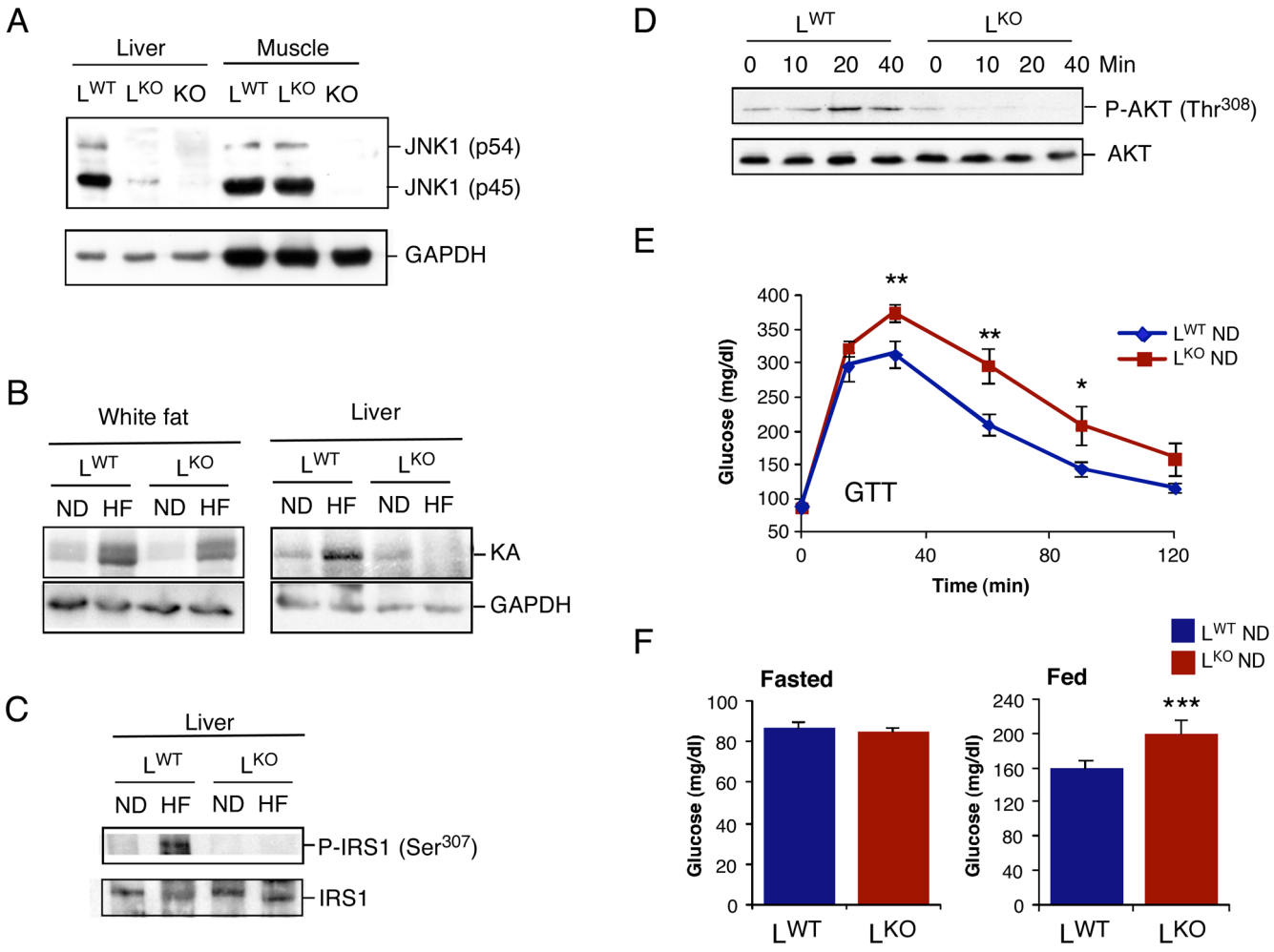

Figure 1. Mice with hepatocyte-specific deficiency of JNK1 are glucose intolerant

(**A**) The liver and quadriceps muscle of *Alb-cre Jnk1*$^{+/+}$ (L^{WT}) mice, *Alb-cre Jnk1*$^{LoxP/LoxP}$ (L^{KO}) mice, and *Jnk1*$^{-/-}$ (KO) mice were examined by immunoblot analysis by probing with antibodies to JNK1 and GAPDH. (**B**) L^{WT} and L^{KO} mice were fed a chow diet (ND) or a high fat diet (HFD) for 16 wks. JNK activity in epididymal (white) fat and liver was measured in a protein kinase (KA) assay using cJun and ATP[γ-^{32}P] as substrates. The cell extracts used for the protein kinase assay were also examined by immunoblot analysis by probing with an antibody to GAPDH. (**C**) The phosphorylation of IRS1 on Ser-307 in the liver was examined using ND- and HFD- fed L^{WT} and L^{KO} mice by immunoblot analysis by probing with antibodies to IRS1 and phosphoSer-307 IRS1. (**D**) Chow- fed L^{WT} and L^{KO} mice were fasted overnight and administered glucose (2g/kg) by intraperitoneal injection. The activation of AKT in the liver was examined by immunoblot analysis by probing with antibodies to AKT and phosphoAKT. (**E**) Glucose tolerance tests of chow-fed L^{WT} and L^{KO} mice were performed by measurement of blood glucose concentration in animals following intraperitoneal injection of glucose (1g/kg). The data presented represent the mean ± SD (n =10 ~ 15). Statistically significant differences are indicated (*, $P < 0.05$; **, $P < 0.01$). (**F**) Chow- fed L^{WT} and L^{KO} mice were fasted overnight or fed *ad libitum* and the blood glucose concentration was measured (mean ± SD; n = 10 ~ 15). Statistically significant differences are indicated (***, $P < 0.001$).

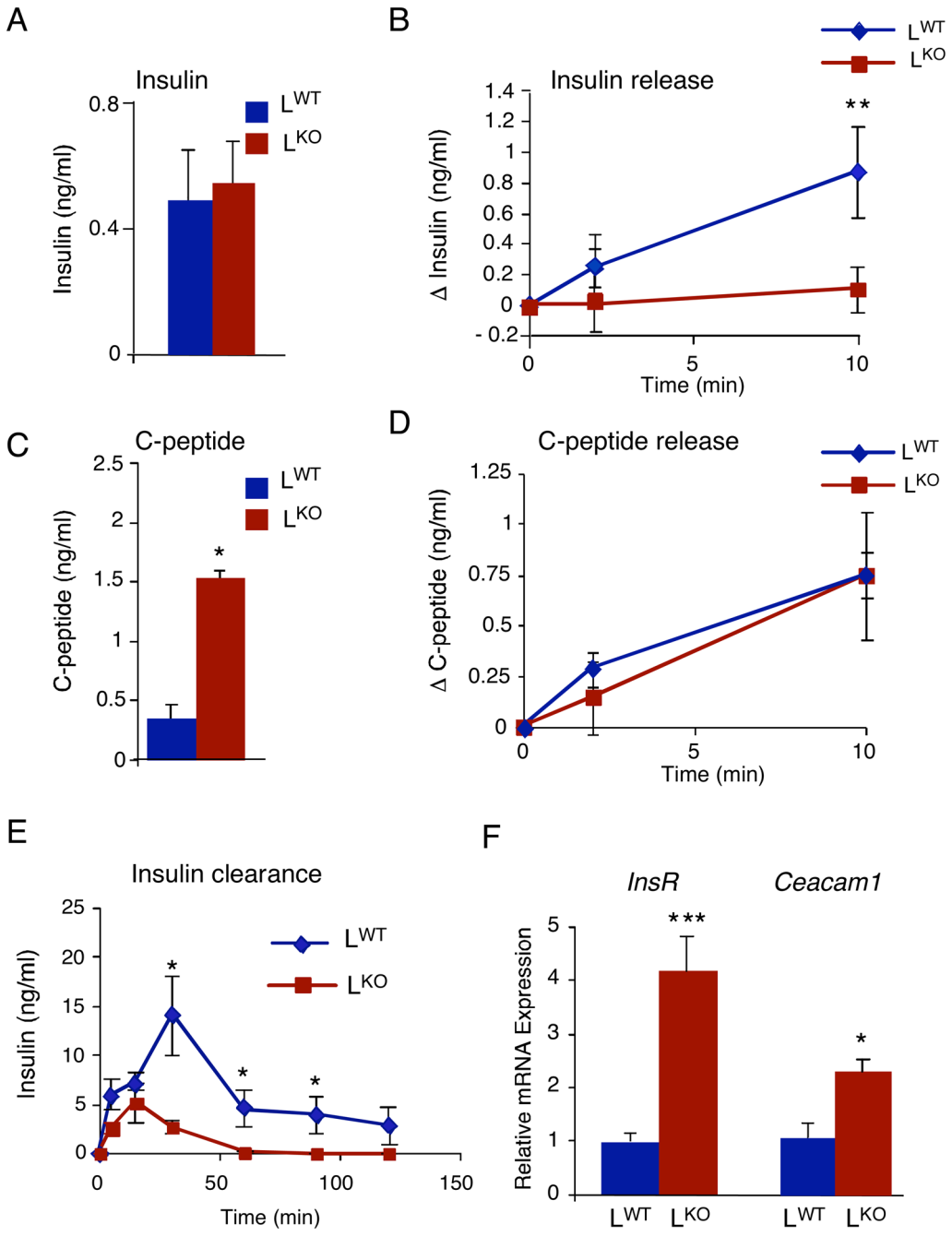

Figure 2. JNK1-deficiency in hepatocytes increases insulin clearance

Chow-fed L^{WT} and L^{KO} mice were fasted overnight. (**A**) The concentration of blood insulin was measured (mean ± SD; n = 10). No statistically significant difference between L^{KO} and L^{WT} mice was detected. (**B**) The effect of administration of glucose (2 g/ kg body mass) by intraperitoneal injection on blood insulin concentration was examined (mean ± SD; n = 13~15). Statistically significant differences between L^{KO} and L^{WT} are indicated (*, $P < 0.01$). (**C**) The concentration of insulin C-peptide in the blood was measured (mean ± SD; n = 10~15). Statistically significant differences between L^{KO} and L^{WT} are indicated (****, $P < 0.0001$). (**D**) The effect of administration of glucose (2 g/kg body mass) on insulin C-peptide concentration in the blood was examined (mean ± SD; n = 15). No statistically significant

difference between L^{KO} and L^{WT} was detected). (**E**) Mice were injected with human insulin (1.5U/kg body mass). The concentration of human insulin in the blood was measured (mean ± SD; n = 15). Statistically significant differences between L^{KO} and L^{WT} are indicated (*, $P < 0.05$). (**F**) The expression of the *insulin receptor*, *Ceacam-1*, and *Gapdh* mRNA in the liver was measured by quantitative RT-PCR (Taqman©) assays. The expression of *insulin receptor* (*InsR*) and *Caecam-1* mRNA was normalized to the amount of *18S* RNA in each sample (mean ± SD; n = 7). Statistically significant differences between L^{KO} and L^{WT} are indicated (*, $P < 0.05$; ***, $P < 0.001$).

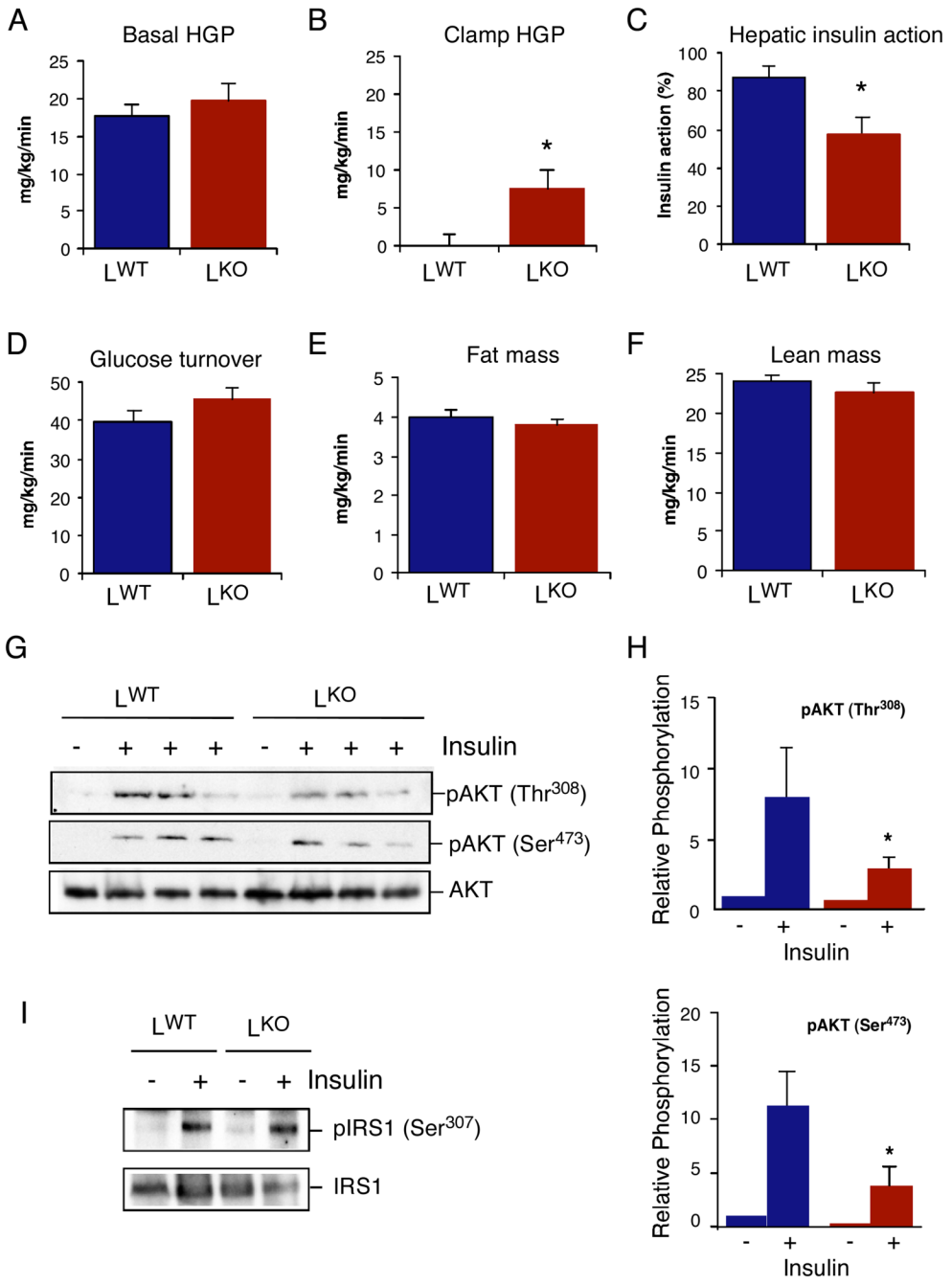

Figure 3. Mice with JNK1-deficient hepatocytes exhibit hepatic insulin resistance

(**A-F**) Insulin sensitivity was measured using a hyperinsulinemic-euglycemic clamp in conscious chow-fed L^{KO} and L^{WT} mice. (A) Basal hepatic glucose production (HGP). (B) Insulin-stimulated rate of HGP. (C) Hepatic insulin action, expressed as insulin-mediated percent suppression of basal HGP. (D) Insulin-stimulated whole body glucose turnover. (E) Whole body fat mass measured using ^{1}H-MRS. (F) Whole body lean mass. The data presented are the mean ± SE for 6 ~ 8 experiments. Statistically significant differences between L^{KO} mice and L^{WT} mice are indicated (*, $P < 0.05$). (**G,H**) Chow-fed L^{KO} and L^{WT} mice were administered insulin (0.3U/kg body mass) by intravenous injection (5 mins). The activation of AKT in the liver was examined by immunoblot analysis by probing with antibodies to AKT

and phosphoAKT. The relative amount of phosphoAKT is presented as the mean ± SD (n = 3). Statistically significant differences between L^{KO} and L^{WT} mice are indicated (*, $P < 0.05$). (**I**) Chow-fed L^{KO} and L^{WT} mice were administered insulin (0.3U/kg body mass) by intravenous injection (5 mins). The phosphorylation of IRS1 on Ser-307 in the liver was examined by immunoblot analysis by probing with antibodies to IRS1 and phosphoSer-307 IRS1.

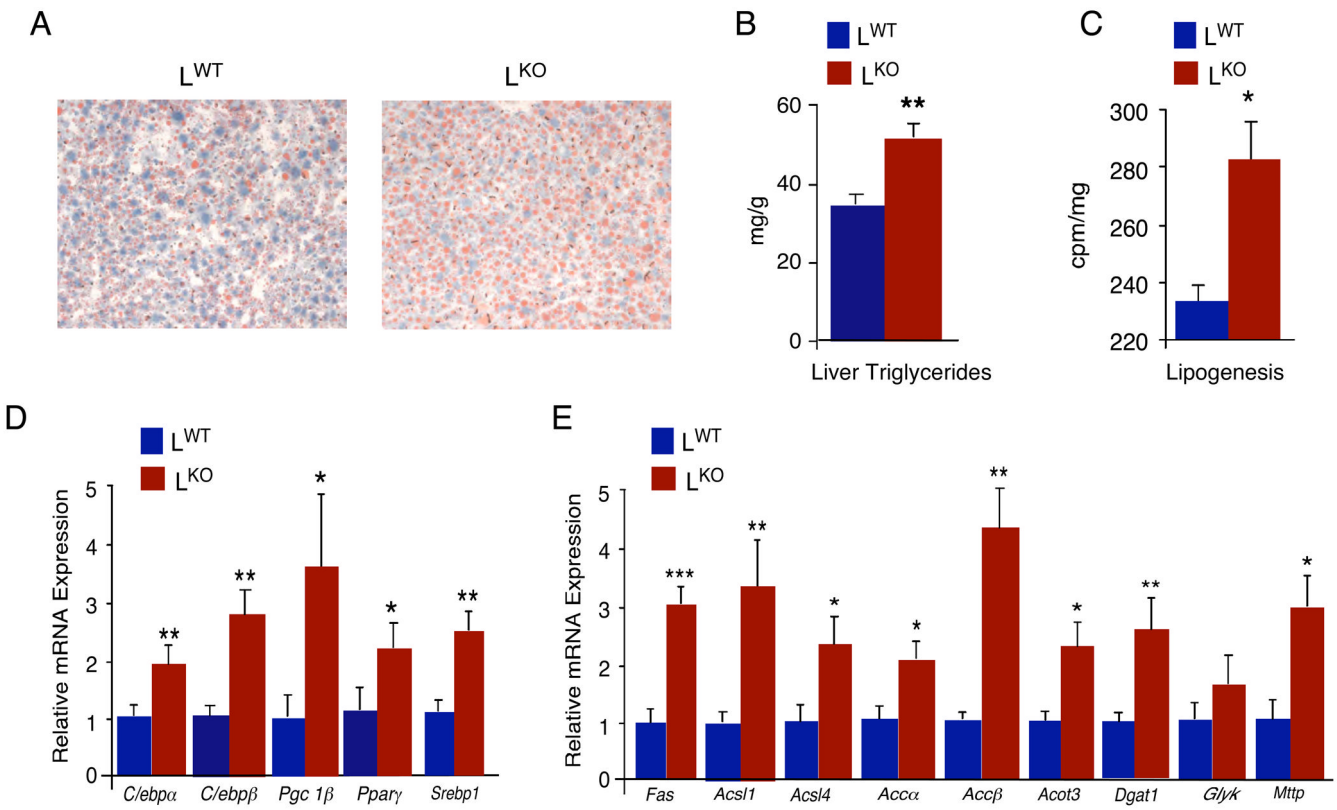

Figure 4. JNK1-deficiency in hepatocytes causes steatosis

(**A**) Chow-fed L^{WT} and L^{KO} mice were fasted overnight. Representative sections of the liver stained with Oil Red-O are presented. (**B**) The amount of hepatic triglyceride was measured in mice fasted over night (mean ± SD; n = 10). Statistically significant differences between L^{KO} and L^{WT} are indicated (*, $P < 0.05$). (**C**) The amount of hepatic lipogenesis was measured in mice fasted 6 hours (mean ± SD; n =8 ~ 9). Statistically significant differences between L^{KO} and L^{WT} are indicated (*, $P < 0.05$). (**D**) The expression of genes that encode lipogenic transcription factors and co-activators in the liver of chow-fed L^{KO} and L^{WT} mice that were fasted overnight (*C/ebpα*, *C/ebpβ*, *Pgc-1β*,*Pparγ*, and *Srebp1*) was measured by quantitative RT-PCR assays of the amount of mRNA and was normalized to the amount of *18S* RNA in each sample (mean ± SD; n = 7). Statistically significant differences between L^{KO} and L^{WT} are indicated (*, $P < 0.05$; **, $P < 0.01$). (**E**) The expression of genes that encode enzymes that promote lipogenesis in the liver of chow-fed L^{KO} and L^{WT} mice that were fasted overnight (*Fas, fatty acid synthase; Acsl1/4, acetyl-CoA synthetase long chain family member 1/4; Acacα/β, acetyl-CoA carboxylaseα/β, Acot3, Acetyl-CoA thioesterase; Dgat1, Diacylglycerol O-acyltransferase homolog 1; Glyk, Glycerol kinase; Mttp, microsomal triglyceride transfer protein*) was measured by quantitative RT-PCR assays of the amount of mRNA and was normalized to the amount of *18S* RNA in each sample (mean ± SD; n = 7). Statistically significant differences between L^{KO} and L^{WT} are indicated (*, $P < 0.05$; **, $P < 0.01$).